

Determination of Bandgap and Energy Band Alignment for High-Dielectric-Constant Gate Insulators Using High-Resolution X-ray Photoelectron Spectroscopy

Hiroshi Itokawa, Tetsuhiro Maruyama, Seiichi Miyazaki and Masataka Hirose.

Department of Electrical Engineering, Hiroshima University

Kagamiyama 1-4-1, Higashi-Hiroshima 739-8527, Japan

phone: +81-824-24-7648 Fax: +81-824-22-7038 e-mail: miyazaki@sxsys.hiroshima-u.ac.jp

1. Introduction

Advanced MOSFETs with gate oxides thinner than 2nm face the problem of significant increase in the direct tunneling leakage current. To avoid this the use of a high-dielectric-constant material such as Ta_2O_5 is thought to be a promising solution. However, a high-dielectric-constant material tends to have a smaller barrier height for electrons[1].

In this work, we have determined the energy bandgaps of high-dielectric-constant materials and the energy band alignment for the $\text{Ta}/\text{Ta}_2\text{O}_5/\text{Si}(100)$ and $\text{TiN}/\text{Ta}_2\text{O}_5/\text{SiO}_2/\text{Si}(100)$ systems by measuring the energy loss spectra of O_{1s} or N_{1s} core levels and the XPS valence band spectra.

2. Experimental

Thin Ta_2O_5 , Si_3N_4 , Al_2O_3 and SiO_2 films were prepared by different procedures as summarized in Table I. The bandgap energies for these films were determined from the onset of the energy loss spectrum for O_{1s} or N_{1s} photoelectrons as schematically explained in Fig. 1[2]. The valence band offset for ultrathin $\text{Ta}_2\text{O}_5/\text{Si}(100)$ and $\text{Ta}_2\text{O}_5/\text{SiO}_2/\text{Si}(100)$ were measured by high-resolution x-ray photoelectron spectroscopy (XPS). The work function of a sputtered TiN film was determined by total photoelectron yield spectroscopy (PYS). Thus the energy band profile for a high-dielectric-constant gate material was determined.

3. Results and Discussion

O_{1s} energy loss spectra for Ta_2O_5 , Al_2O_3 and SiO_2 and N_{1s} loss spectrum for Si_3N_4 are compared in Fig. 2. The photoexcited electrons suffer inelastic losses due to plasmon and the band-to-band excitation as shown in Figs. 1 and 2. The plasmon loss signal exhibits a rather broad peak at 22 ~ 25 eV away from the O_{1s} or N_{1s} core level energies for SiO_2 , Al_2O_3 and Si_3N_4 , and at ~ 15 eV for Ta_2O_5 . The onset of the electron excitation from the valence to conduction bands can be also observed at an energy separated by the bandgap energy from the core level peak as seen in Fig. 2. The bandgaps determined from the threshold energy of the energy loss spectra in Fig. 2 are summarized in Table II, where the accuracy of the measurements is ± 0.05 eV. All the measured values are

consistent with the reported data for bulk films as determined by photoinjection or photoconductivity measurements[3-8].

In order to determine the energy band profile for a high-dielectric-constant gate material, the XPS valence band spectrum was measured for the 5.2 nm-thick $\text{Ta}_2\text{O}_5/\text{Ta}$ system as shown in Fig. 3. Since the valence band spectrum is composed of a mixture of the density of states (DOS) for Ta_2O_5 and Ta, it can be deconvoluted by using the valence band spectra separately measured for Ta and Ta_2O_5 as indicated in Fig. 3. From the energy difference between the valence band tops of Ta_2O_5 and Ta, the valence band alignment is obtained to be 4.20 eV. Considering the Ta_2O_5 bandgap of 4.65 eV (Fig. 1), the electron barrier height for the $\text{Ta}_2\text{O}_5/\text{Ta}$ system is 0.45 eV as illustrated in Fig. 4. Taking into account the energy difference between the $\text{Si}(100)$ valence band maximum and the vacuum level being 5.15 eV as determined by the photoelectron yield spectrum[9], the electron barrier height in the $\text{Ta}_2\text{O}_5/\text{Si}(100)$ interface is evaluated to be 0.28 eV.

In order to directly confirm this band alignment, the valence band spectrum for Ta_2O_5 evaporated on the hydrogen-terminated, atomically flat $\text{Si}(100)$ surface was measured as shown in Fig. 5. Since the free energy for the oxide formation from Ta is smaller than that from Si, the Ta_2O_5 layer on Si can be reduced by Si to form an ultrathin SiO_2 layer at the interface. The top of the valence band DOS for SiO_2 thermally grown on $\text{Si}(100)$ appears at the binding energy deeper than 4.49 eV from the top of the $\text{Si}(100)$ valence band[10], while the Ta_2O_5 valence band spectrum emerges from ~ 3.0 eV with respect to the top of the $\text{Si}(100)$ valence band as shown in Fig. 5. Therefore, there is no measurable SiO_2 layer formed at the evaporated $\text{Ta}_2\text{O}_5/\text{Si}(100)$ interface in the spectrum of Fig. 5. By subtracting the contribution of the $\text{Si}(100)$ DOS measured for a hydrogen-terminated $\text{Si}(100)$ surface from the observed valence band spectrum for the $\text{Ta}_2\text{O}_5/\text{Si}(100)$ system, the valence band alignment at the $\text{Ta}_2\text{O}_5/\text{Si}(100)$ interface is determined to be 3.25 eV as indicated in Fig. 5. Using the measured valence band offset and the bandgap energies for Ta_2O_5 and Si, the conduction-band barrier height at the $\text{Ta}_2\text{O}_5/\text{Si}(100)$ interface is obtained to be 0.28 eV as illustrated in

Table I. Fabrication procedures of gate dielectrics.

Gate Dielectrics	Process Condition	Thickness (nm)	Substrate
Ta_2O_5	Chemical Oxidation	5.2	pure-Ta
	Thermal Oxidation (500°C)	≥ 10.0	
	$\text{Ta}(\text{OC}_2\text{H}_5)_5 + \text{O}_2$ [LPCVD]	5.0	
	$\text{Ta}_2\text{O}_5 + \text{O}_2$ [Evaporation]	4.5	
Si_3N_4	$\text{SiH}_2\text{Cl}_2 + \text{NH}_3$ [LPCVD]	3.0	Si(100)
Al_2O_3	Al [Evaporation] + Thermal Oxidation	5.5	
SiO_2	Thermal Oxidation (1000°C)	2.0~5.0	

Table II. The energy bandgap E_g of gate dielectrics.

Gate Dielectrics		E_g from XPS (eV)	E_g for Bulk Film (eV)
Ta_2O_5	Chemical Oxidation	4.85	4.2~5.2 [3,4]
	Thermal Oxidation	4.65	
	CVD	4.75	
	Evaporation	4.65	
Si_3N_4	CVD	4.75	4.5~4.7 [5]
Al_2O_3	Thermal Oxidation	6.55	5.6~6.7 [6,7]
SiO_2	Thermal Oxidation	8.95	8.9~9.0 [8]

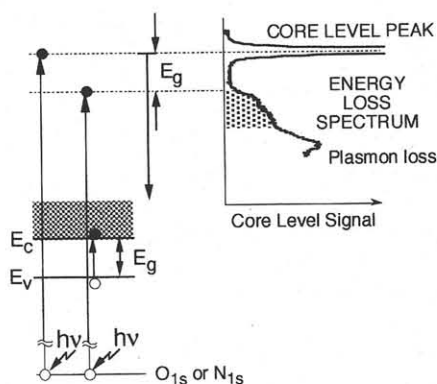


Fig. 1 Determination of bandgap energy for dielectric materials by O_{1s} or N_{1s} photoelectron energy loss spectrum.

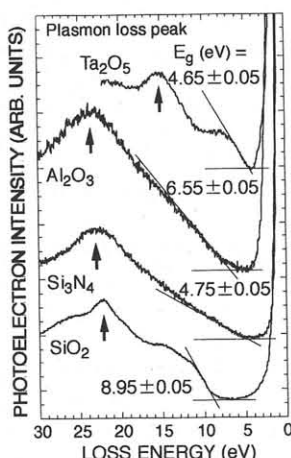


Fig. 2 Energy loss spectra for Ta_2O_5 , Al_2O_3 , Si_3N_4 and SiO_2 .

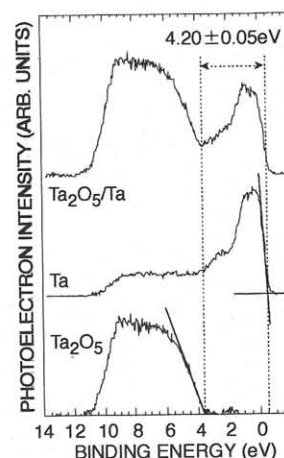


Fig. 3 Valence band spectrum for the Ta_2O_5/Ta system and the deconvoluted spectra for Ta and Ta_2O_5 .

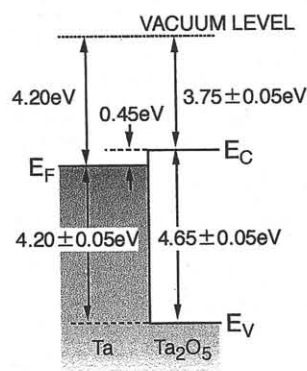


Fig. 4 Energy band profile for the Ta_2O_5/Ta system.

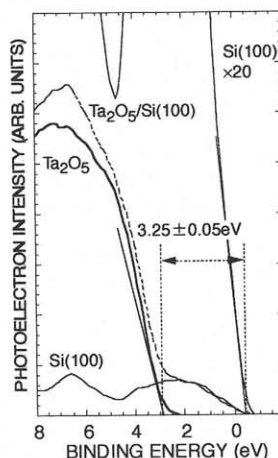


Fig. 5 Valence band spectrum for the evaporated $Ta_2O_5/Si(100)$ system and the deconvoluted spectra for Ta_2O_5 and hydrogen-terminated $Si(100)$ surface.

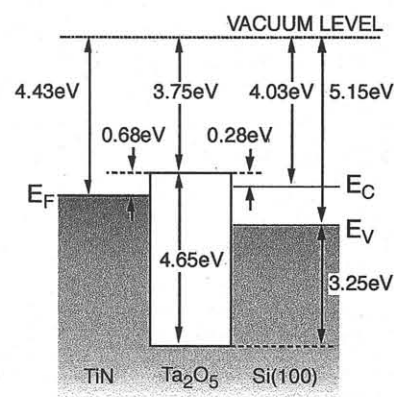


Fig. 6 Energy band profile for the $TiN/Ta_2O_5/Si(100)$ system.

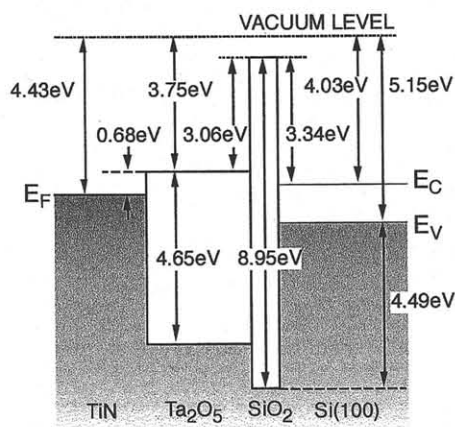


Fig. 7 Energy band profile for the $TiN/Ta_2O_5/SiO_2/Si(100)$ system.

Fig. 6. This agrees well with the estimated value from the result of Fig. 4. Also, the barrier height at the TiN/Ta_2O_5 interface is determined to be 0.68 eV, where the TiN work function was obtained by total photoelectron yield spectrum. From these results the energy band profile for the $TiN/Ta_2O_5/SiO_2/Si(100)$ system can be determined as shown in Fig. 7.

4. Conclusions

It is demonstrated that the energy band profile for the metal/high-dielectric-constant gate insulator/ $Si(100)$ system can be accurately determined from the energy loss spectrum of the

core level photoelectrons for the insulator combined with the corresponding XPS valence band density of states.

Acknowledgment

Part of this work was supported by the "Research for the Future" Program in the Japan Society for the Promotion of Science (No. RFTF96R13101).

References

- [1] S. A. Campbell et al., IEEE Trans. Electron Devices, **44**, 104 (1991).
- [2] S. Miyazaki et al., Appl. Surf. Sci., **113/114**, 585 (1997).
- [3] W. H. Knausenberger et al., Jpn. J. Electrochem. Soc., **120**, 927 (1973).
- [4] P. A. Murawala et al., Jpn. J. Appl. Phys., **32**, 368 (1993).
- [5] H. R. Phillip, Jpn. J. Electrochem. Soc., **120**, 259 (1973).
- [6] P. D. Edward, Handbook of Optical Constants of Solids II, (ACADMIC PRESS, INC. 1991) p. 761.
- [7] A. M. Goodman, Appl. Phys. Lett., **41**, 2176 (1970).
- [8] T. H. Distefano et al., Solid State Commun., **9**, 2259 (1971).
- [9] S. Miyazaki et al., Mat. Sci. in Semiconductor Processing (1999) to be published.
- [10] J. L. Alay and M. Hirose, J. Appl. Phys. **81**, 1606 (1997).